https://erjm.journals.ekb.eg
ISSN: 1110-1180

DOI: ---------

ERJ
Engineering Research Journal
Faculty of Engineering
Menoufia University

Assessment of Applying Demand Side Management Techniques on Distribution Networks Performance: A Practical Case

Heba A. Khattab[1], Fatma F. Awad [2, *], Asmaa F. Nasef [1]

[1] Department of Electrical Eng., Faculty of Eng., Menoufia University, Egypt.
[2] M. Sc. Candidate, Department of Electrical Eng., Faculty of Eng., Menoufia University, Egypt.
**(Corresponding author: pepomer2020@gmail.com)*

ABSTRACT
In the last decade, there has been a great interest in applying Demand Side Management (DSM) actions in electric power systems as an alternative to constructing and operating new capacity generation units. Also, DSM allows customers to make decisions that affect their energy consumption, which reduces peak-hour energy providers' demand and reshapes the load profile. This paper proposes a methodology for applying load reduction results from DSM techniques to electric power networks. This methodology uses sensitivity analysis to select the buses on which the load reduction will be performed. Furthermore, changes in hourly system loading are considered, and the impacts of these variations on the system's performance are analyzed. Also, the Monte Carlo Simulation (MCS) methodology has been utilized to consider the load uncertainties. The DSM has been effectively validated on two power distribution networks. The first is the IEEE 33 standard system, while the second is a practical distribution network, which is Shebin El Kom feeder-Menoufia Governorate South Delta Electricity Company. Different indicators are used to assess the enhancement of the network's performance. Simulation results concluded that applying DSM techniques reduced the power taken from the substation, reduced the active power losses, and improved the minimum voltage with the daily loading variation as well as at peak loading.

Keywords: *DSM; Loading uncertainty; MV distribution networks; Active power losses; Voltage profile*.

1. Introduction

Traditionally, electrical energy is produced from major power plants and delivered to consumers by transmission and distribution networks. The rapidly growing electricity consumption around the world, especially in Egypt, is due to development needs and an increasing population [1, 2]. According to the annual report of the Egyptian Ministry of Electricity and Renewable Energy for the year 2020/2021, the maximum electrical load during peak hours increased from 25.71 GW in 2012 to 28.02 GW in 2015 to 30.8 GW in 2018 and increased to 34.1 GW in 2022 (an increase of 8.98%, 9.94%, and 10.7%, respectively) [3]. Therefore, the Electrical distribution networks will suffer a series of pressures as electricity demand becomes faster than electric power generation. Also, due to the distance between power plants and consumers and the lack of continuous communication between the power utility and consumers, the performance of power grids deteriorated [4,5]. Furthermore, aging infrastructure leads to continuous maintenance of the grid structure. Also, among the problems of overloading of lines are an increase in system power losses and the reduction of voltage regulation, efficiency, reliability, quality, and safety [1, 2, 4, 5, 6]. According to the previous challenges, utility companies are forced to treat these problems by different methods.

To dissolve the previous challenges there are many common alternates such as distributed generation (DG), storage systems, capacitor banks (CB), load reduction, and demand-side management (DSM) [6, 7, 8]. DG, CB, and storage systems are the most expensive technologies and may not be suitable to match available generation with demand in some cases, while load shedding or load curtailment is indispensable to prevent any network overloading. However, the customers cannot accept this since supply continuity represents an essential need for them [5, 9,10-13]. Otherwise, loads can be fully controllable by implementing DSM during peak hours and increasing the utilization factor with a cost reduction. The chance to raise power system efficiency and decrease the high cost of the power system has been the key driver behind introducing DSM [1, 2]. DSM is

a necessary technique that can warrant the feasible and economical operation of any power distribution system [14, 15].

DSM is one of the low-cost ways to improve the performance of distribution systems compared to other solutions [1, 2, 6, 16]. DSM is the promising method for utilities to delay building further capacity by reducing peak electricity demand as it is the set of methodologies for adjusting load consumption patterns so that demand is limited within supply and gives consumers an opportunity to save money by lowering their electricity bills [17]. In addition, controlling peak demand for networks may improve the overall performance of the system as it results in reduced power losses, enhanced voltage regulation, and improved overall system efficiency and reliability. In addition, DSM can reduce power line overload and stop service interruptions. These advantages can be obtained without the wastage of consumers' necessities [6, 15-17].

Recently, different forms of the DSM have been applied by network operators to control the load profiles of the system and to enhance system generation-load balancing [18]. The DSM can be divided into popular six techniques such as Direct Load Control (DLC) which utilities can shut down certain loads during peak hours to avoid system meltdown. Also, Load Shifting (LS) shifts loads from peak to off-peak hours while Energy Efficiency (EE) decreases the overall energy consumption by replacing normal appliances with energy-efficient appliances. Furthermore, Peak clipping, flexible load shape, and valley filling are used to reduce peak and fill the off-peak demands, respectively [10, 15].

Numerous articles on the DSM of Smart Grids (SG) have been published; these studies mostly address distributed generation with integration of renewable energy, demand response (DR) load scheduling that is optimum, and innovative enabling technologies and systems [4, 7, 11, 16]. Also, Numerous articles on the DSM of Smart Grids (SG) have been published; these studies mostly address the available optimization approaches for applying DSM [8, 9, 19].

A new smart load management approach is presented in [6], that the programming part is necessary for the load management control centers. The results attained verify the efficacy and efficiency of the approach that was developed to address the issue of overloading, improve network performance, and satisfy customer needs. The suggested technique was applied to a really overloaded Egyptian distribution network. In [13], the DSM was applied to enhance the performance of power systems using sensitivity factors to classify the load centers according to their priority to determine suitable demand reduction levels. The IEEE 30 bus system is used to highlight the demand-side management strategy under different loading conditions. In [18], authors presented the concept of load forecasting a day in advance as a forecasted curve and then analyzed the load curve using evolutionary algorithms to shift loads and reshape the load profile in real-time simulations. In [20], the DSM is an essential methodology in planning future grids that convert end-user energy consumption based on financial incentives. Authors in [21], presented the strategy of an energy management system–based demand response scheduling in a distributed power system for minimization of customer bills and network losses. This paper proposes a methodology for applying load reduction (LR) as one technique of DSM techniques to distribution power networks. This methodology uses sensitivity analysis to select the buses on which the load reduction will be performed. Furthermore, changes in hourly system loading (load uncertainties) are considered, and the impacts of these variations on the system's performance are analyzed.

The key contributions of this study are as follows:

- Sensitivity analyses were performed to determine the worst and most effective feeders for applying demand-side management actions to enhance distribution network performance.
- Two levels of applying load reduction are handled and added to that, the uncertainties in loading values are investigated.
- The DSM is effectively validated on two power distribution networks: the IEEE 33 standard system and a practical distribution network (Shebin El Kom feeder-Menoufia Governorate South Delta Electricity Company).
- For all cases, active and reactive power losses are significantly reduced while the voltage profile of all distribution nodes is improved.

This paper is arranged into 6 sections as follows: the modeling of the systems is investigated in section 2. In section 3, the proposed solution methodology is presented. Section 4 discusses the obtained simulation res. Section 5 illustrates the discussion of the results. Section 6 elaborates on the paper's conclusions.

2. Systems Modelling

2.1 Load Modelling

In recent years, there has been an increase in interest in load modeling, and power system load has become a new field for exploring power system stability. The power system load model is a series of mathematical equations that define the relationship between active and reactive power, voltage, and frequency at a certain bus bar in a system [22].

The load class data is frequently categorized as residential, commercial, industrial, and agricultural. The residential load contains most of the equipment associated with housing habits, as well as a significant proportion of electric heating and air conditioning systems throughout the winter and summer seasons, respectively. Commercial loads include air conditioners and a substantial percentage of discharge lighting, whereas agricultural loads are induction motors used to drive pumps. The industrial load is mostly associated with industrial operations, and most of the load, up to 95%, refers to industrial motors and electric heating procedures, like soldering, which may be used in heavy industries.

Furthermore, many types of loads in power systems are static, while others are dynamic in nature; for example, most customers have lighting, cooling, and heating equipment, etc. Because of this variation of loads, power system operation desired models of loads to be accurately estimated, to make a credible decision on the distribution network and evaluate the power consumption of a typical infrastructure [22]. Most of the load models are assorted as static sources of active and reactive powers. It is independent of voltage magnitude and known as the constant-power load model. A load, on the other hand, can be modeled as a constant-current or constant-impedance source [23]. In the constant-current source model, the active and reactive powers of the load fluctuate linearly with voltage magnitude, but they vary quadratically with voltage magnitude in the constant-impedance model. The following are the mathematical equations for the real active and reactive powers of a load for the three models mentioned above [22-25]

$$P = \mathrm{P}_o * \left(\frac{v_i}{v_o}\right)^{\mu} \quad (1)$$

$$\mathrm{Q} = \mathrm{Q}_o * \left(\frac{v_i}{v_o}\right)^{\mu} \quad (2)$$

Where P_o and Q_o are the initial active power and reactive load power at the nominal voltage, respectively. v_i is the magnitude of real bus voltage while v_o is the rated voltage and equals 1.0 PU. μ = 0, 1, and 2 represent the constant-power, constant-current, and constant-impedance load models.

2.2 Distribution Feeder Modelling

The conductors are not straight wires, but strands of wire that have been twisted together to produce a single conductor with increased tensile strength. An aluminum conductor, steel reinforced (ACSR) is a common type of conductor. The internal core is made of steel strands, while the outside layer is made of two layers of aluminum strands. Other conductor types in use include all aluminum conductors (AAC), all aluminum alloy conductors (AAAC), aluminum conductors, and alloy reinforced (ACAR). In general, the standard π model is a wide term for modeling a distribution line joining two nodes. The conductor resistance, self, and mutual inductive reactance make up the series impedance of single-phase or three-phase distribution lines. The resistor value depends on the conductor quality expressed by the company. Also, the inductive reactance (self and mutual) component of the impedance is described by the following equation as a function of the total magnetic fields surrounding a conductor [2].

$$\lambda_i = 2.10^{-7} * (I_1 . ln\frac{1}{D_{i1}} + I_2 . ln\frac{1}{D_{i2}} + \cdots + I_i . ln\frac{1}{GMR_i} + \cdots + I_n . ln\frac{1}{D_{in}}) \quad W - {}^{T}/_{m} \quad (3)$$

Where

Din, GMR_i are the distance between conductor i and conductor n (ft), and the Geometric mean radius of conductor i (ft), respectively.

The inductance of conductor i is formatted as the conductor's self-inductance and the mutual inductance between the conductor i and all the other n-1 conductors.

By definition,

$$Self - Inductance: L_{ii} = \frac{\lambda_i}{I_i} = 2 * 10^{-7} * \ln\frac{1}{GMR_i} \quad H/m \quad (4)$$

$$Mutual\ Inductance: L_{in} = \frac{\lambda_{in}}{I_n} = 2 * 10^{-7} * \ln\frac{1}{D_{in}} \quad H/m \quad (5)$$

2.3 Test Systems Description

In this study, two distribution networks are studied. The single-line diagrams of both networks are shown in Fig. 1. The first system is IEEE 33 standard system which consists of 33 nodes with 32 lines. It has 3.715 MW and 2.3 MVAr loading, and its rated voltage is 12.66 kV [26-28]. Its initial active power losses, reactive power losses, efficiency, and voltage regulation are 211 kW, 143.03 kVAr, 94.62%, and 10.647%, respectively. It is worth noting that the first system consists of four lateral feeders, namely: feeder_1 from bus No. 7 to bus No. 18; feeder_2 from bus No. 3 to bus No. 25; feeder_3 from bus No. 6 to

bus No. 33, and feeder_4 from bus No. 2 to bus No. 22, as shown in Fig.1a. The second system is Shebin El Kom feeder-Menoufia Governorate South Delta Electricity Company which is a real one. It consists of 28 nodes with 27 lines. It has 2.160 MW and 1.03 MVAr loading, and its rated voltage is 11 kV. Its initial active power losses, reactive power losses, efficiency, and voltage regulation are 82.79 kW, 28.94 kVAr, 94%, and 9.5%, respectively. This system consists of three lateral feeders, namely: feeder_1 from bus No. 2 to bus No. 5; feeder_2 from bus No. 7 to bus No. 12, and feeder_3 from bus No. 6 to bus No. 28, as shown in Fig. 1b. All buses and feeders' data of the real system are listed in the Appendix.

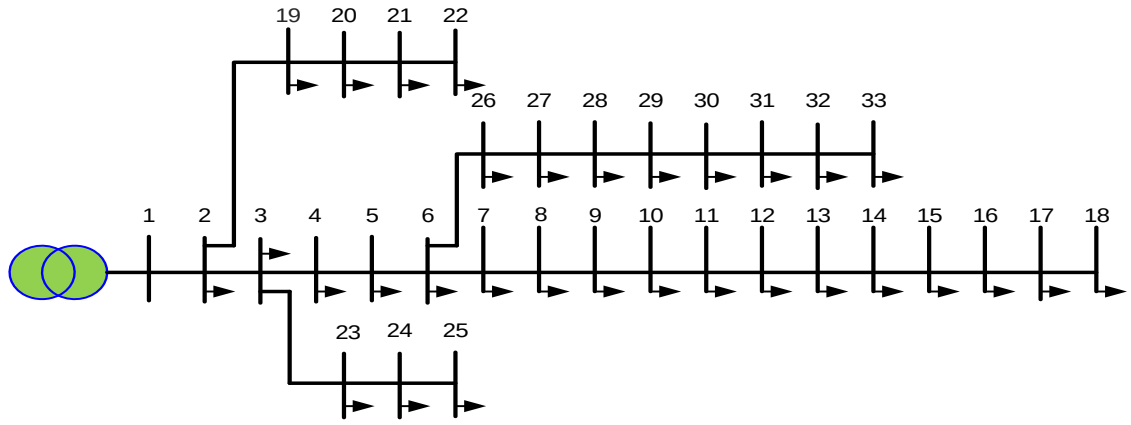

(a) IEEE 33 bus distribution network

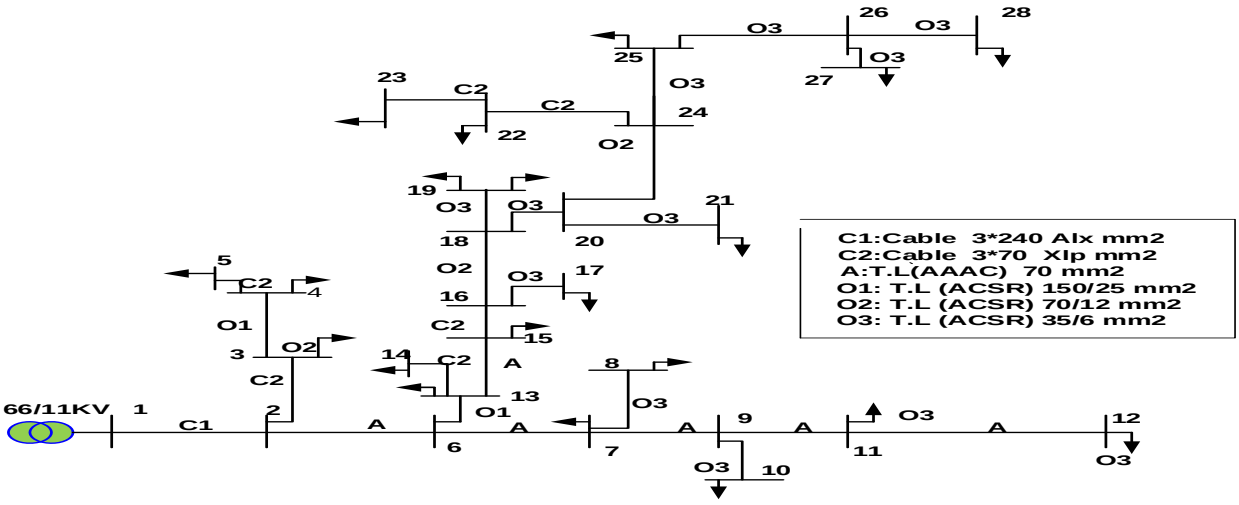

Egyptian Real Distribution network

Fig. 1 Single-line diagram of the two studied networks

3. Proposed Solution Methodology

The more sensitive buses for the system have been determined by the sensitivity procedure as follows [13]:

1. Firstly, the value of a certain load is changed from (S_I) to ($S_I + \Delta S_I$), while the values of other loads remained unchanged.

2. Then calculate all transmission lines power flowing ΔS_{TL-ij}.

3. The sensitivity factor for each bus i "SF_i" is defined using the following equation (6):

$$SF_i = \frac{\sum_{i=0}^{n} \Delta S_{TL-ij}}{\Delta S_i} \quad (6)$$

4. The buses are classified according to their sensitivity factor in descending order [11].

5. Buses are classified into best and worst buses according to the sensitivity factor value of buses. The best bus is the bus whose sensitivity factor value is the highest while the worst bus is the bus whose sensitivity factor value is the lowest.

By applying the previous sensitivity procedure:

- The obtained SF values are ranked in descending order as illustrated in Tables 1 and 2 for the two studied power systems. Also Figs. 2a and 2b show the SF values for all buses of the first and the second systems, respectively.
- Based on the results from Tables 1 and 2 and Figs. 2a and 2b, it can be concluded that bus 18 and bus 22 in the first and second systems, respectively have the highest SF values, and hence, it presents suitable locations for demand reduction which results from applying DSM techniques.
- Bus 2 and bus 7 in the first and second systems, respectively have the lowest SF values.

Table 1 Ranked SF values for IEEE 33 bus system

Bus No.	S.F	Rank	Bus No.	S.F	Rank
18	0.2433	1	28	0.1468	17
17	0.2349	2	7	0.1269	18
14	0.2285	3	27	0.1241	19
16	0.2281	4	26	0.118	20
13	0.2176	5	6	0.1113	21
15	0.214	6	25	0.0729	22
32	0.2017	7	5	0.0713	23
33	0.2009	8	24	0.0634	24
12	0.2001	9	4	0.0548	25
31	0.1957	10	23	0.0453	26
11	0.1952	11	3	0.037	27
10	0.1889	12	22	0.0192	28
29	0.1764	13	21	0.0175	29
30	0.1758	14	20	0.0157	30
9	0.173	15	19	0.0075	31
8	0.1639	16	2	0.0064	32

Table 2 Ranked SF values for the real system

Bus No.	S.F	Rank	Bus No.	S.F	Rank
22	0.3193	1	**13**	0.2122	11
27	0.3178	2	**5**	0.2066	12
28	0.3174	3	**4**	0.2051	13
23	0.3169	4	**3**	0.2050	14
25	0.3101	5	**11**	0.1997	15
21	0.2991	6	**12**	0.1913	16
19	0.2816	7	**10**	0.1228	17
17	0.2764	8	**8**	0.1068	18
15	0.2275	9	**7**	0.0867	19
14	0.2193	10			

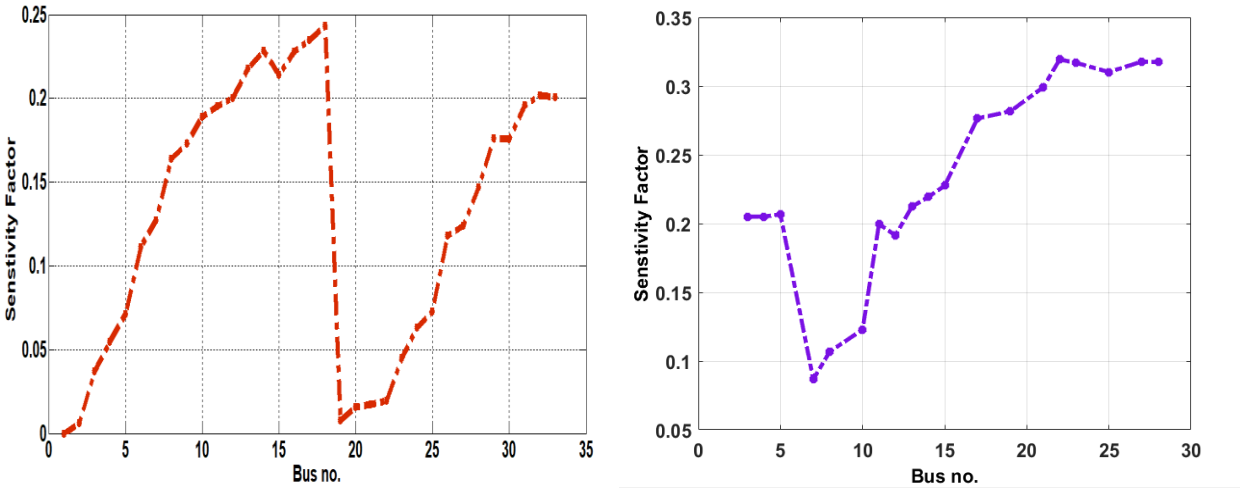

(a) Standard IEEE 33 bus system (b)An Egyptian real distribution system

Fig. 2 SF values versus bus numbers

To validate the results of SF and to determine the best and the worst feeders, the load reduction of 20% is applied to all lateral feeders separately in both systems.

- It appears that the best lateral feeder for IEEE 33 bus system is feeder_1 from bus No. 7 to bus No. 18 and the worst lateral feeder is feeder_4 from bus No. 2 to bus No. 22 in terms of reducing system active power losses with different loading throughout the day hours as shown in Fig. 3a.
- Also, the best lateral feeder for the real system is feeder_3 from bus No. 6 to bus No. 28 and the worst feeder is feeder_2 from bus No. 7 to bus No.12 in terms of reducing system active power losses with different loading throughout the day hours as shown in Fig. 3b.
- The best feeder contains the best bus (the highest SF value) and the worst feeder contains the worst bus (the lowest SF value) for the two studied power systems. Therefore, these feeders are the suggested feeders to apply load reduction on them.

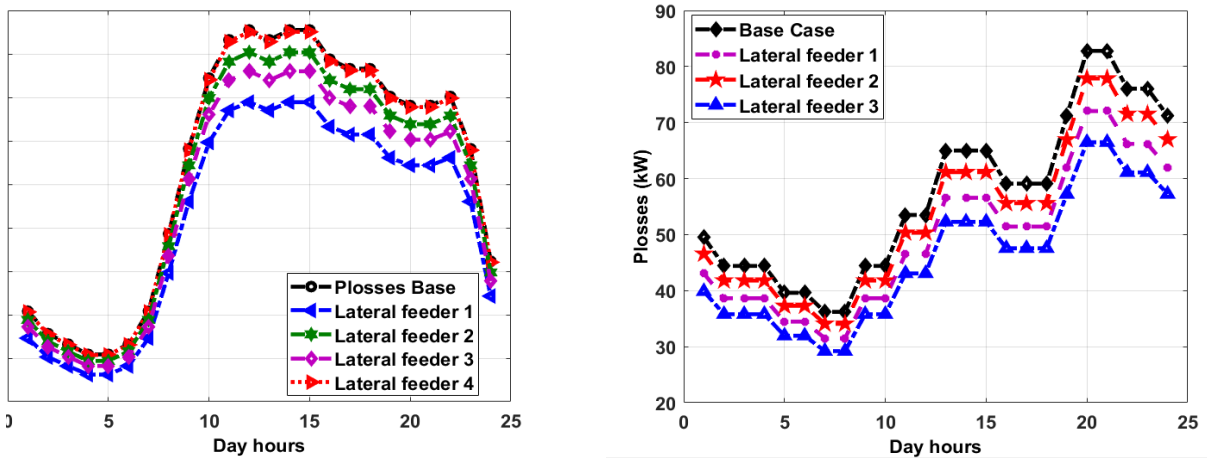

a) P_{losses} of IEEE 33 bus system b) P_{losses} of the real power system

Fig. 3 Daily variation of P_{losses} for applying 20% load reduction to every lateral feeder in both systems.

4. Simulation Results

In this study, three cases are investigated to study the effect of load reduction on the system's performance. The first case is implemented by reducing all load centers of the selected feeder by 20%. The second case is implemented by reducing all load centers of the selected feeder by 30%. Each case has three scenarios as follows:

- **Scenario (1):** Applying load reduction on the worst feeder.
- **Scenario (2):** Applying load reduction on the best feeder.
- **Scenario (3):** Applying load reduction for half of the best feeder including the sensitive bus.

The effect of these cases and scenarios are studied on the power drawn from the grid (P_{grid}), systems active power losses (P_{losses}), and systems voltage profile as shown in the following subsections. The third case is to study the uncertainties of the load by using Monte Carlo Simulation.

A. Case 1

The effect of applying the three scenarios is shown in Figs. 4-10. Fig. 4 shows the daily variation of the P_{grid} for the three scenarios compared with the base case for the two studied power systems. It can be observed from Figs. 4a and 4b that applying 20% load reduction reduced P_{grid} for all scenarios but with different reduction percentages. It can be observed that the reduction in P_{grid} is even more remarkable for scenario 2 than the other scenarios for the two studied power systems. Also, the peak loading hours occurred at 12 pm, 2 pm, and 3 pm for IEEE 33 bus system while 8 p.m. and 9 p.m. for the real power system.

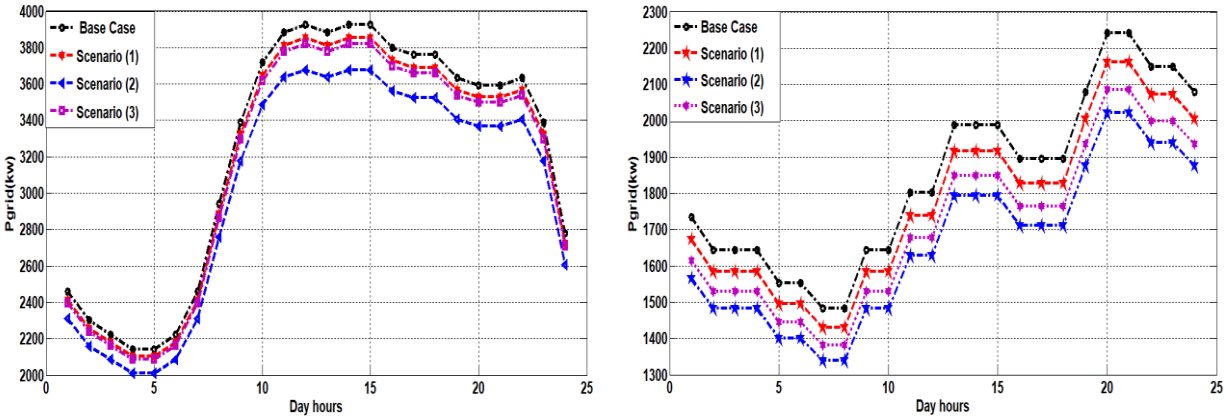

a) P_{grid} for IEEE 33 bus system

b) P_{grid} for the real power system

Fig. 4 Daily variation of the power from the grid for case 1

Figs. 5a and 5b show P_{grid} at peak loading for the three scenarios compared to the base case. From Fig. 5a, it can be seen that P_{grid} for the first system is reduced from 3.926 MW to 3.853 MW, to 3.678 MW, and to 3.819 MW with reduction percentages of 1.85%, 6.3%, and 2.7% for scenarios 1, 2, and 3 compared with the base case. And from Fig. 5b, it can be seen that P_{grid} for the second system was reduced from 2.243 MW to 2.163 MW, to 2.023 MW, and to 2.086 MW with reduction percentages of 3.5%, 9.8%, and 6.9% for scenarios 1, 2, and 3 compared with the base case. Therefore, it's concluded that the best scenario is scenario 2 which represented the application of load reduction on the best feeder.

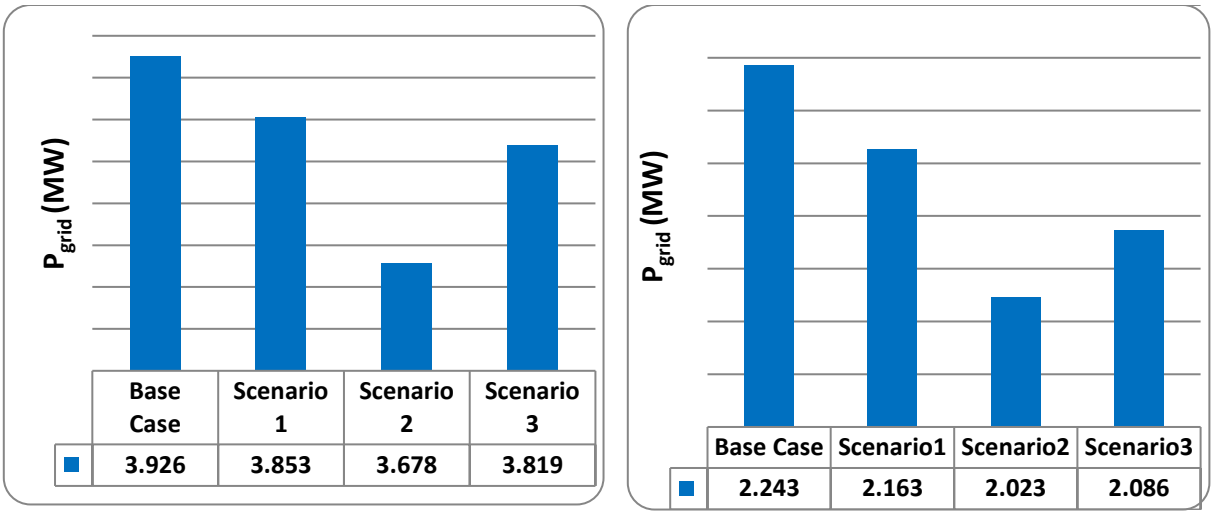

a) P_{grid} for IEEE 33 bus system b) P_{grid} for the real power system

Fig. 5 Power drawn from the grid for case 1 during the peak loading

The daily active power losses variations for the three scenarios compared to the base case for the two studied power systems are shown in Figs. 6a and 6b. These figures illustrated the effectiveness of applying demand reduction in reducing the P_{losses} of the two studied power systems during the day.

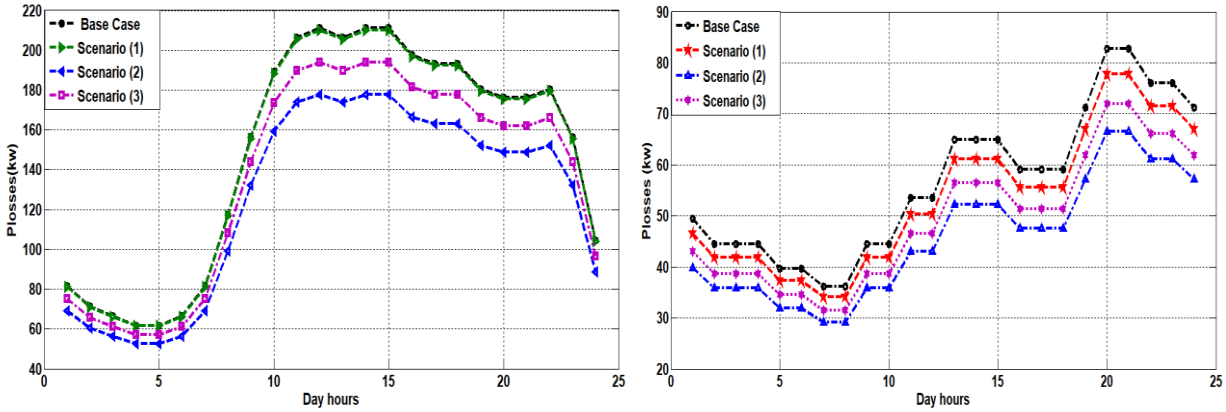

c) P_{losses} of IEEE 33 bus system d) P_{losses} of the real power system

Fig. 6 Daily variation of the active power losses for case 1

Figs. 7a and 7b show P_{losses} for case 1 during peak loading for the first and second systems, respectively. From Fig. 7a, it can be seen that P_{losses} of the first system is reduced from 211 kW to 210 kW to 177.8 kW, and to 193.9 kW with reduction percentages of 0.47%, 15.7%, and 8.1% for scenarios 1, 2, and 3 compared with the base case. And from Fig. 7b, it can be seen that P_{losses} of the second system is respectively reduced from 82.79 kW to 77.86 kW, to 66.48 kW, and to 71.89 kW with reduction percentages of 5.9%, 19.7%, and 13.16% for scenarios 1, 2, and 3 compared with the base case. It is clear from the results that the reduction in P_{losses} is even more pronounced for scenario 2 than the other scenarios for the two studied power systems.

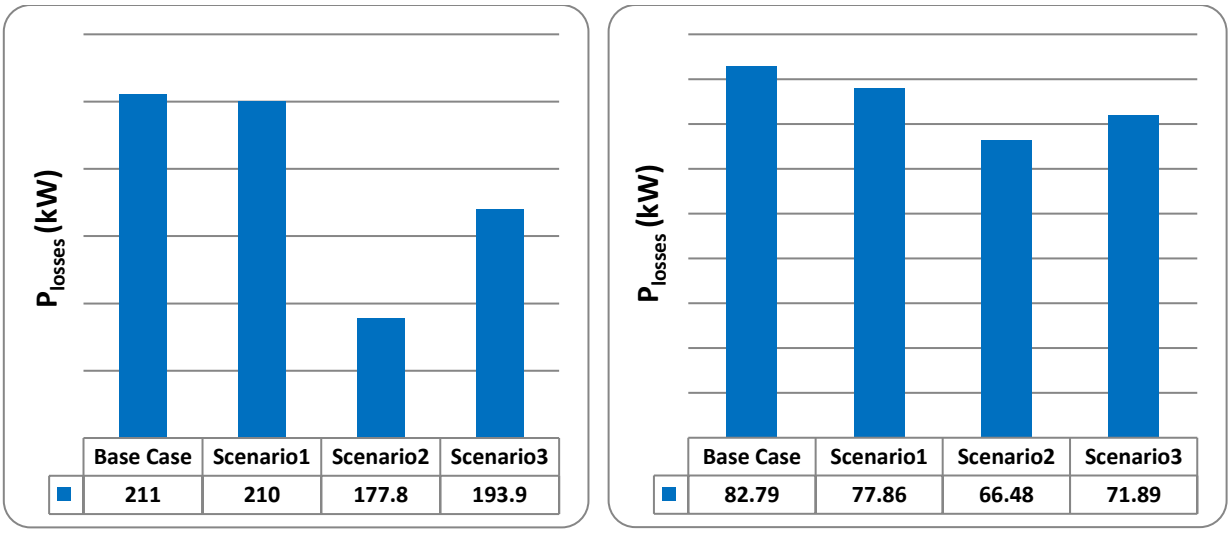

a)P_{losses} of IEEE 33bus b) P_{losses} of the real power system

Fig. 7 Active power losses for case 1 during the peak loading

The daily variations of the bus with minimum voltage for the three scenarios compared with the base case for the two studied power systems are shown in Figs. 8a and 8b. Fig. 8a shows the daily variation of voltage at bus 18 which is the minimum bus voltage of the first system. It illustrated the effectiveness of applying demand reduction in improving the minimum voltage with the daily loading variation. Also, the daily variation of voltage at bus 22 which is the minimum bus voltage of the second system is shown in Fig. 8b under applying the three scenarios in case 1. These figures illustrated that scenario 2 is more effective where the minimum voltage increased by a large percentage compared with the base case during the day hours rather than the others scenarios.

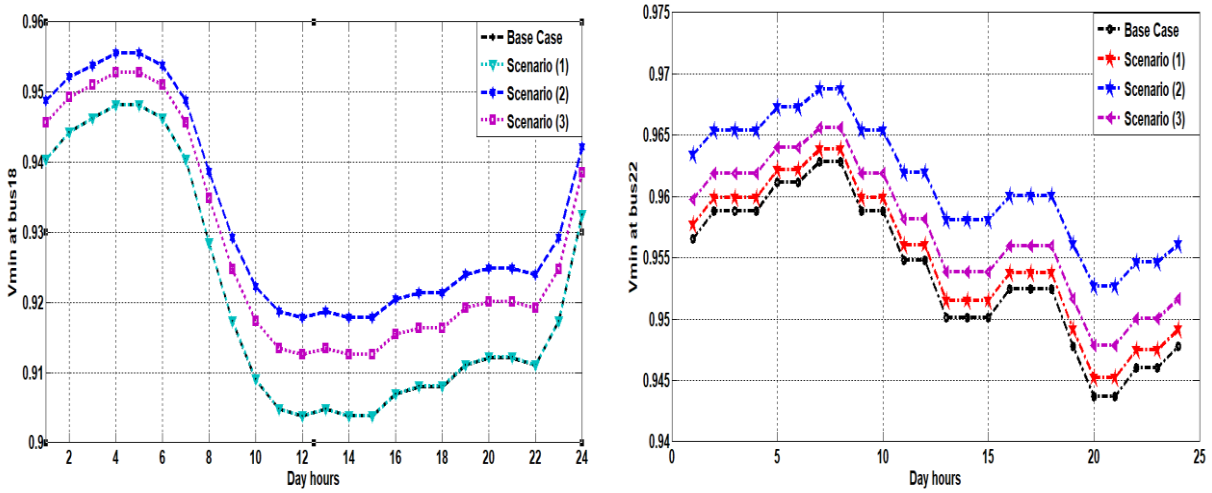

a) Voltage at bus 18 for IEEE 33bus b) Voltage at bus22 for the real power system

Fig. 8 Daily variation of the minimum voltage bus for case 1

Figs. 9a and 9b show the minimum voltage V_{min} for case 1 during peak loading for the first and second systems, respectively. From Fig. 9a, it can be seen that the voltage at bus 18 for the first system remains constant as its base value for scenario 1, and increased from 0.9038 PU to 0.9178 PU, and to 0.9126 PU by an improvement percentage of 1.5%, and 0.96 % for scenario 2, and scenario 3 compared with the base case, respectively. Also, Fig. 9b shows the voltage at bus 22 for the second system at the peak loading. It increased from 0.9437 PU to 0.9452 PU, to 0.9527,

and to 0.9465 by an improvement percentage of 0.15%, 0.95%, and 0.295% for scenarios 1, 2, and 3 compared with the base case, respectively. The best scenario for improving the minimum voltage bus of the two studied systems is scenario 2. Figs. 10a and 10b show the system voltage profile for the two studied power systems under applying case 1 for the three scenarios during the peak load of the systems. These figures show the extent of improvement that occurred in the systems voltage buses, especially the minimum voltage buses, with the application of demand reduction particularly scenario 2.

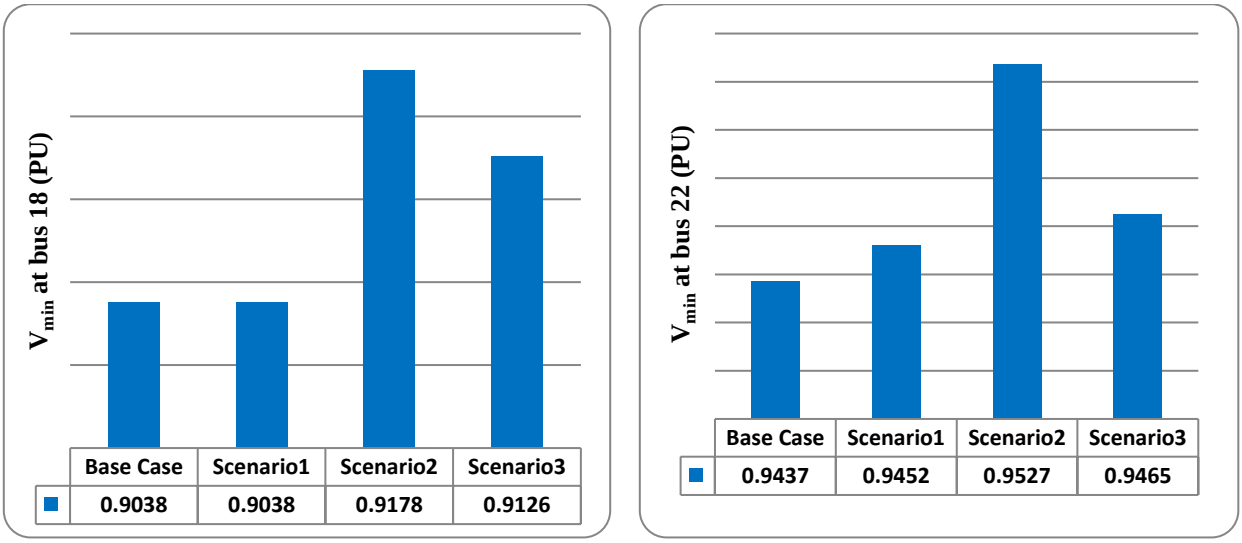

a) Voltage at bus18 IEEE 33bus b) Voltage at bus22 the real power system

Fig .9 Minimum voltage for case 1 during the peak loading

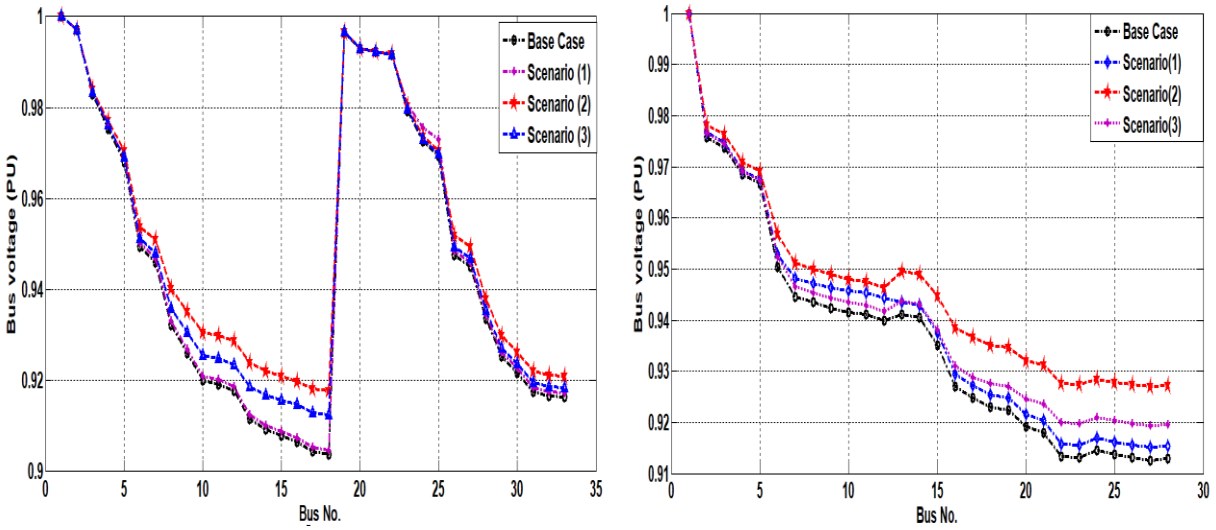

a)Voltage profile of IEEE 33 bus b)Voltage profile of the real power system

Fig .10 Voltage Profile for case 1 during the peak loading

B. Case 2

The effect of applying the previous scenarios is shown in Figs. 11-17. Fig. 11 shows the daily variation of the P_{grid} for the three scenarios compared to the base case for the two studied power systems. It can be observed from Figs. 11a and 11b that applying 30% load reduction reduced P_{grid} for scenarios 2, 3, and 1, respectively with different reduction percentages. It can be noticed that the reduction in P_{grid} is even more salient for scenario 2 than the other scenarios for the two studied power systems.

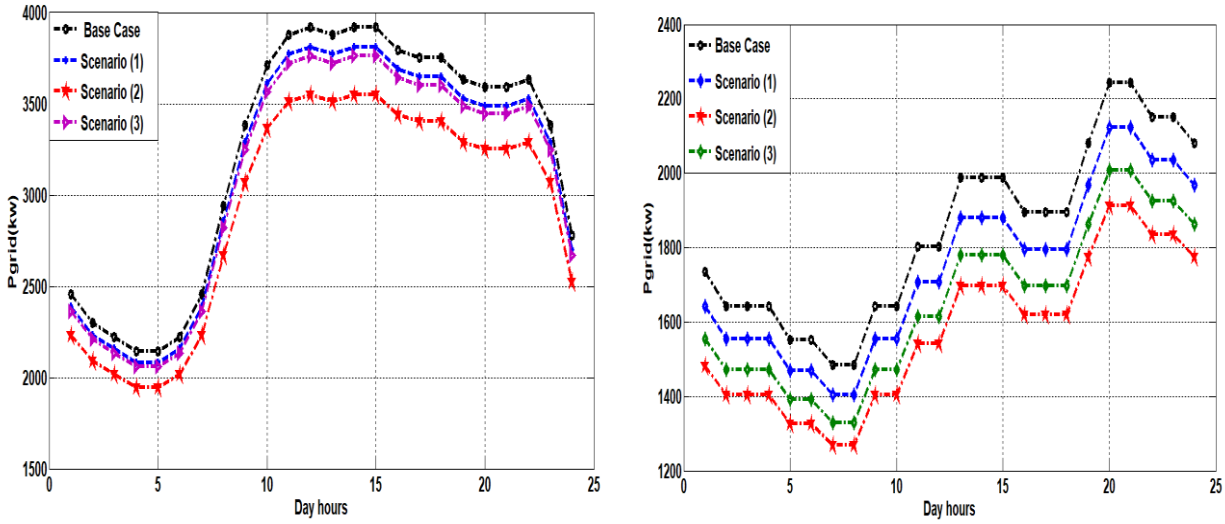

a) P_{grid} for IEEE 33 bus system b) P_{grid} for the real power system

Fig. 11 Daily variation of the power drawn from the grid for case 2

Figs. 12a and 12b show P_{grid} during systems peak loading for the three scenarios in case 2 compared to the base case. From Fig. 12a, it can be seen that P_{grid} for the first system is reduced from 3.926 MW to 3.817 MW, to 3.556 MW, and to 3.766 MW with reduction percentages of 2.7%, 9.4%, and 4.07% for scenarios 1, 2, and 3 compared with the base case. And from Fig. 12b, it can be seen that P_{grid} for the second system is reduced from 2.243 MW to 2.123 MW, to 1.914 MW, and to 2.008 MW with reduction percentages of 5.3%, 14.6%, and 10.47% for scenarios 1, 2, and 3 compared with the base case. So, it's concluded that the best scenario, in this case, is scenario 2 which represented the application of load reduction on the best feeder according to the proposed methodology.

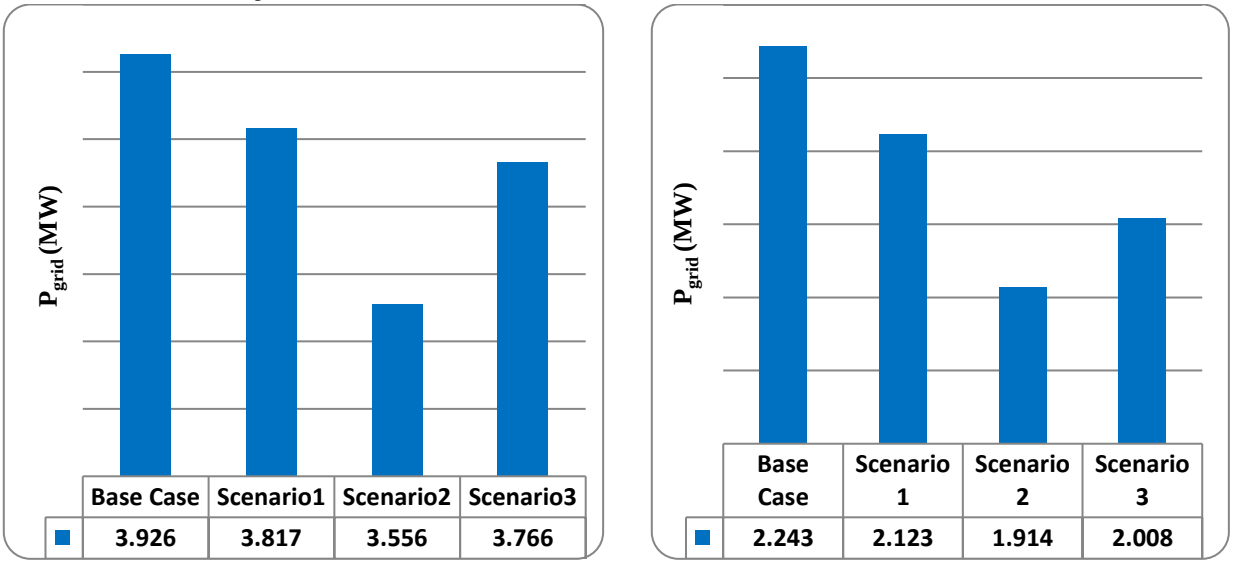

a) P_{grid} for IEEE 33 bus system b) P_{grid} for the real power system

Fig. 12 Power drawn from the grid for case 2 during the peak loading.

The daily variation of P_{losses} for the three scenarios compared to the base case for the two studied power systems is shown in Figs. 13a and 13b. These figures illustrated the effectiveness of applying demand reduction in reducing the P_{losses} in the two studied power systems during the day.

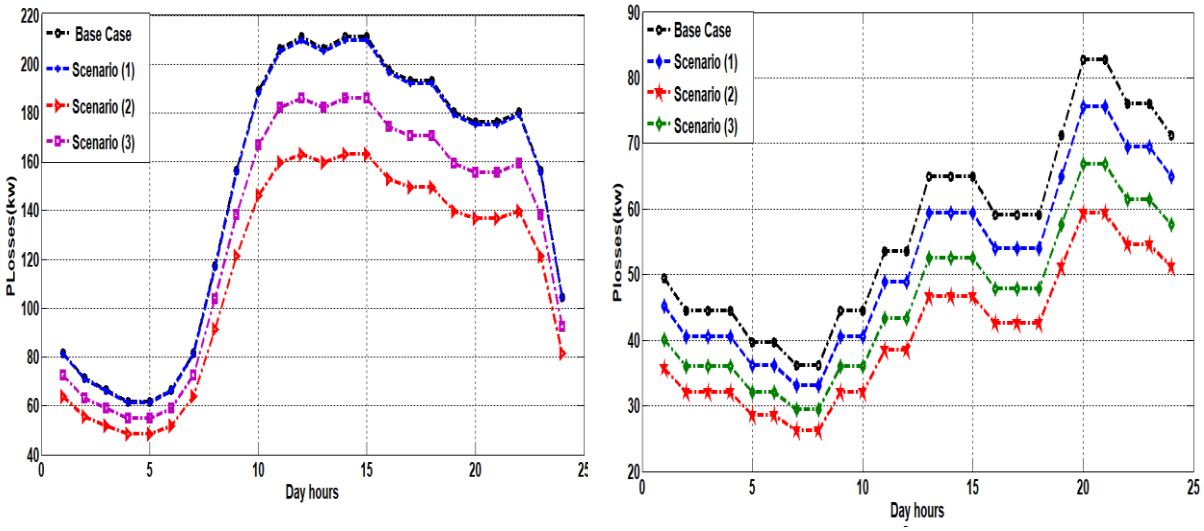

a) P_{losses} of IEEE 33 bus system b) P_{losses} of the real power system

Fig. 13 Daily variation of the active power losses for case 2

Figs. 14a and 14b show the P_{losses} for case 2 during peak loading for the first and second systems, respectively. From Fig. 14a, it can be seen that P_{losses} for the first system is reduced from 211 kW to 209.8 kW, to 163.2 kW, and to 186 kW with reduction percentages of 0.57%, 22.7%, and 11.8% for scenarios 1, 2, and 3, respectively compared with the base case. And from Fig. 14b, it can be seen that P_{losses} for the second system is reduced from 82.79 kW to 75.54 kW, to 59.38 kW, and to 66.88 kW with reduction percentages of 8.7%, 28.27%, and 19.2% for scenarios 1, 2, and 3, respectively compared with the base case. It is clear from the results that the reduction in the active power losses is even more pronounced in scenario 2 for the two studied power systems.

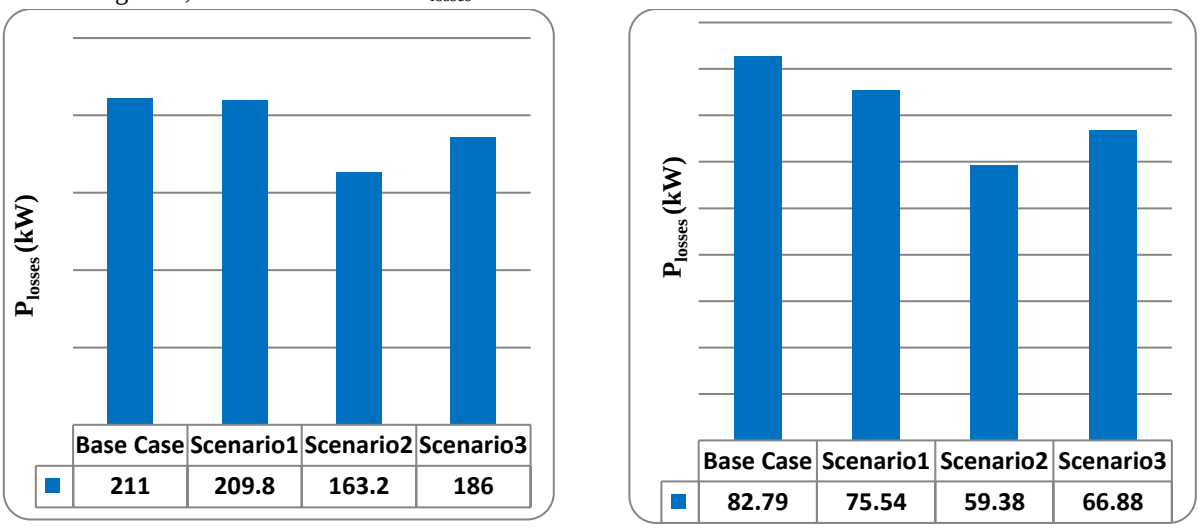

a) P_{losses} of IEEE 33bus b)P_{losses} of the real power system

Fig. 14 Active power losses for case 2 during the peak loading

The daily minimum voltage Vmin variations for the three scenarios compared to the base case for the two studied power systems are shown in Figs. 15a and 15b. Fig. 15a shows the daily variation of voltage at bus 18 which is the minimum bus voltage of the first system. It illustrated the effectiveness of applying demand reduction in improving the minimum voltage with the daily loading variation. Also, the daily variation of voltage at bus 22 which is the minimum bus voltage of the second system is shown in Fig. 15b under applying

the three scenarios in case 2. These figures illustrated that scenario 2 is more effective where the minimum voltage increased by a large percentage compared with the base case during the day hours rather than the others scenarios.

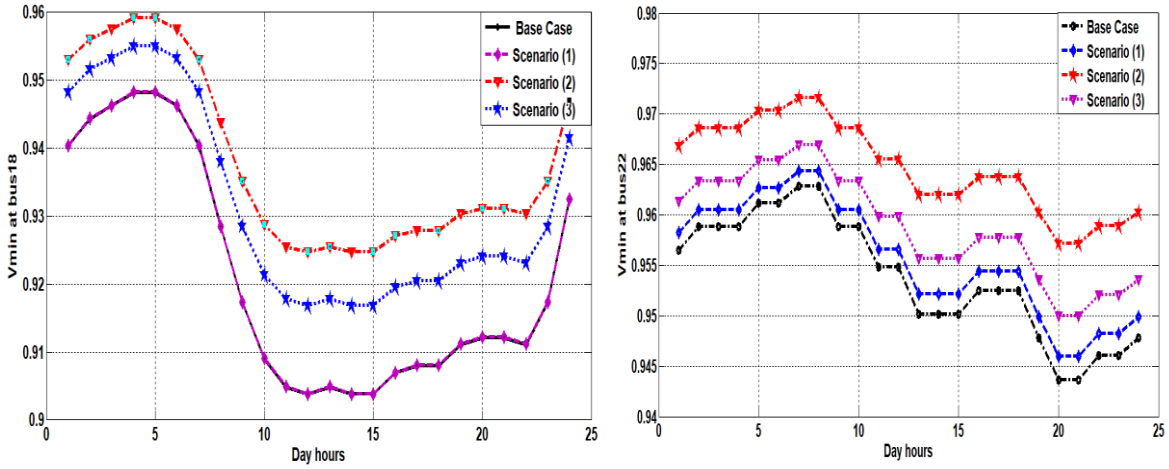

a) Voltage at bus18 for IEEE 33bus b) Voltage at bus 22 for the real power system

Fig.15 Daily variation of the minimum voltage bus for case 2

Figs. 16a and 16b show the minimum voltage for case 2 during peak loading for the first and second systems, respectively. From Fig. 16a, it can be seen that the voltage at bus 18 for the first system remains almost constant in its base value in the case of scenario 1, and increased from 0.9038 PU to 0.9247 PU and to 0.9169 PU by an improvement percentage of 2.26% and 1.4 % for scenarios 2 and 3 compared with the base case, respectively. Also, Fig. 16b shows the voltage at bus 22 for the second system at the peak loading. It increased from 0.9437PU to 0.946 PU, to 0.9572, and to 0.951 by an improvement percentage of 0.24%, 1.4%, and 0.76 % for scenarios 1, 2, and 3 compared with the base case, respectively. The best scenario for improving the minimum voltage bus of the two studied systems is scenario 2. Figs. 17a and 17b show the system voltage profile for the two studied power systems under applying case 2 for the three scenarios during the peak load of the systems. These figures show the extent of improvement that occurred in the systems voltage buses, especially the minimum voltage buses, with the application of demand reduction in different scenarios.

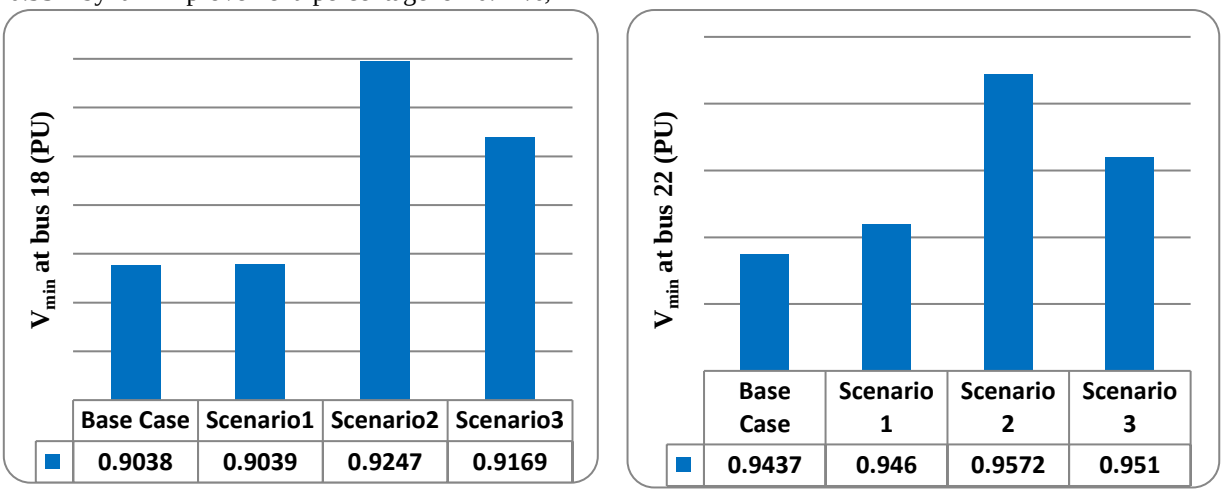

a) Voltage at bus18 IEEE 33bus b) Voltage at bus22 the real power system

Fig .16 Minimum voltage for case 2 during the peak loading

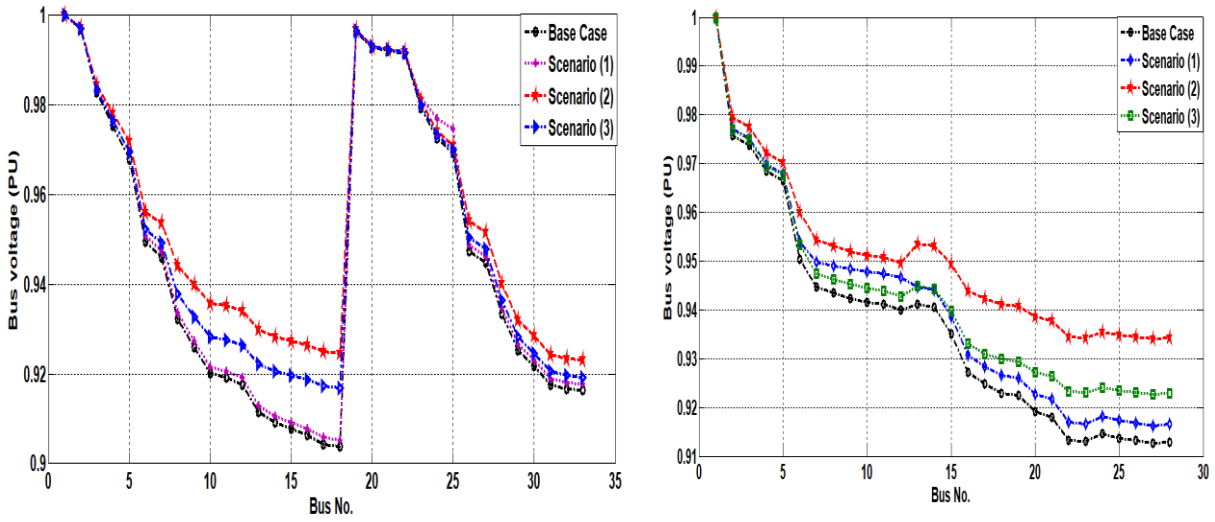

a)Voltage profile of IEEE 33 bus b) Voltage profile of the real power system

Fig .17 Voltage Profile for case 2 during the peak loading

C. Case 3

The Monte Carlo Simulation (MCS) methodology has been applied to study the load uncertainties. 1000 scenarios are created around the maximum loading condition in the two studied power systems, which is 100 % based on the MCS [29]. In addition, three groups of loads A, B, and C are considered with three various standard deviations of 3, 5, and 8%, respectively. Three **Scenario**s are studied for the maximum loading condition:

- **Scenario** 1: MCS with the base case.
- **Scenario** 2: MCS with a 20% reduction in loading of the best feeder.
- **Scenario** 3: MCS with a 20% reduction in loading of the worst feeder.

For **Scenario 1**: Active power losses and voltage at bus 18 are recorded in Figs. 18a and 18b as histogram figures under maximum load conditions. In Fig. 18a, the active power losses are in the range [195-220] kW with a probability of 58.6% while the maximum probability percentage of 12.7% is prospective to the active power losses of 210 kW. In addition, the maximum and minimum active power losses are prospective to be 260 kW and 175 kW with a probability of 0.2% and 1.2%, respectively.

The voltage at bus 18 is in the range [0.901-0.907] PU with a probability of 73.4% whereas the maximum probability percentage of 16.1% is prospective with a value of 0.9035 PU as shown in Fig. 18b. In addition, the maximum and minimum expected values of the voltage at bus 18 are 0.911 PU and 0.896 PU with a probability of 1.4% and 0.3%, respectively.

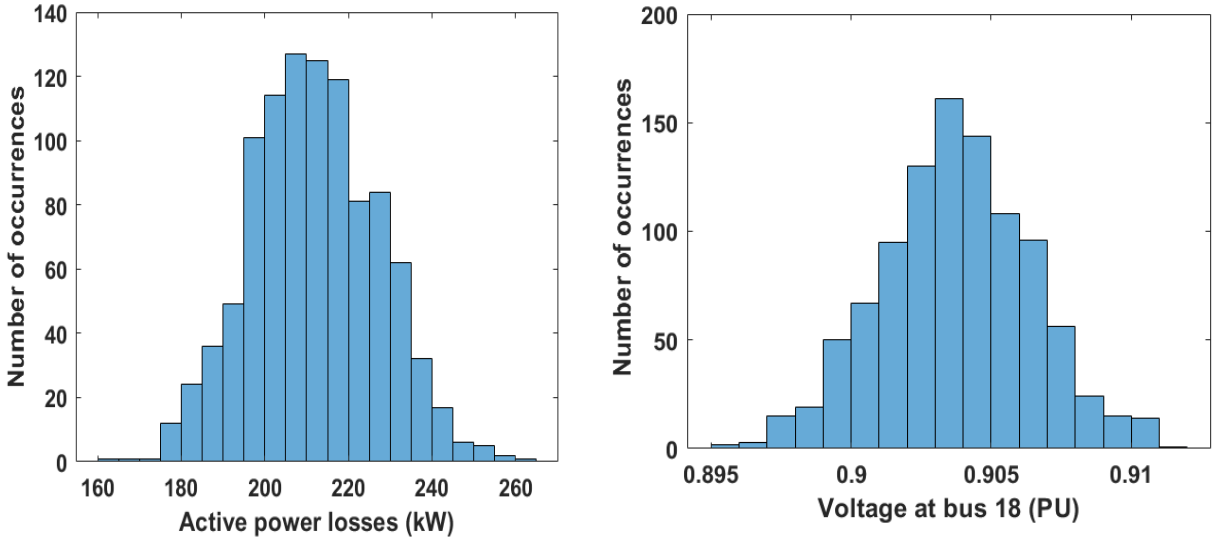

a) Active power losses b) Per unit volatge at the minimum voltage bus

Fig. 18 Number of occurrences of the results for Scenario 1 for the first system

For **Scenario 2:** The histograms of the active power losses and the voltage at bus 18 are recorded as shown in Figs. 19a and 19b under maximum loading conditions. Fig. 19a shows the system's active power losses where they are in the range [165-190] kW with a probability of 61% whereas the maximum probability percentage of 14.5% is prospective with active power losses of 172 kW. In addition, the maximum and minimum active power losses are prospective to be 220 kW and 140 kW with a probability of 0.3% and 0.4%, respectively.

The voltage at bus 18 is in the range [0.915-0.92] PU with a probability of 68.8% whereas the maximum probability percentage of 17.6% is prospective with a value of 0.918 PU as shown in Fig. 19b. In addition, the maximum and minimum expected values of the voltage at bus 18 are 0.925 PU and 0.91 PU with a probability of 0.3% and 0.3%, respectively.

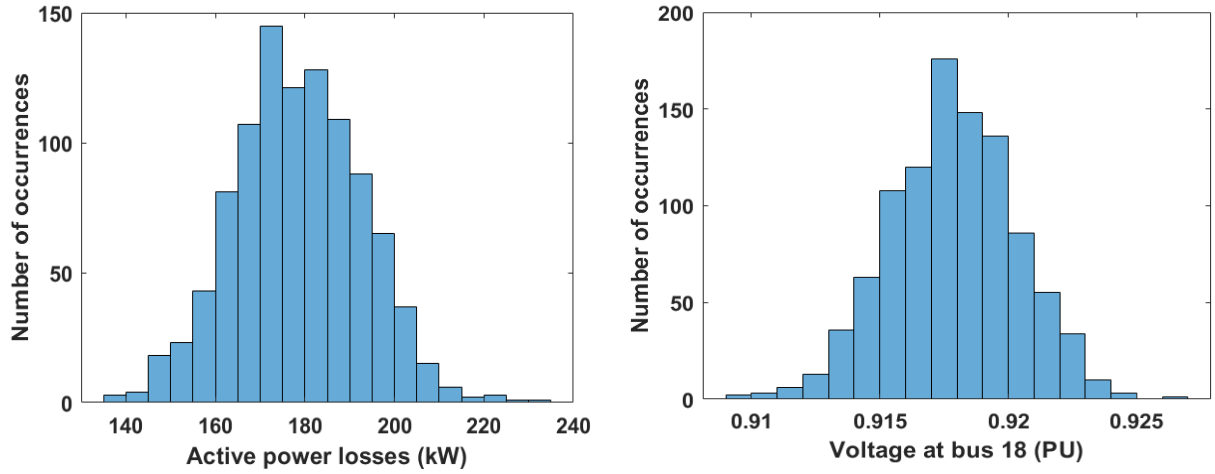

a) Active power losses b) Per unit volatge at the minimum voltage bus

Fig. 19 Number of occurrences of the results for the first system for Scenario 2

For **Scenario** 3: The histograms of active power losses and voltage at bus 18 are recorded as shown in Figs. 20a and 20b, respectively under maximum loading conditions. The active power losses are in the range [195-225] kW with a probability of 66% where the maximum probability percentage of 14.9% is prospective with active power losses of 212 kW as shown, in Fig. 20a. In addition, the maximum and minimum active power losses are prospective to be 260 kW and 170 kW with a probability of 0.4% and 0.4%, respectively.

The voltage at bus 18 is in the range [0.901-0.906] PU with a probability of 63.7% whereas the maximum probability percentage of 14.5% is prospective with a value of 0.902 PU as shown in Fig. 20b. In addition, the maximum and minimum expected values of the voltage at bus 18 are 0.911 PU and 0.895 PU with a probability of 0.2% and 0.6%, respectively.

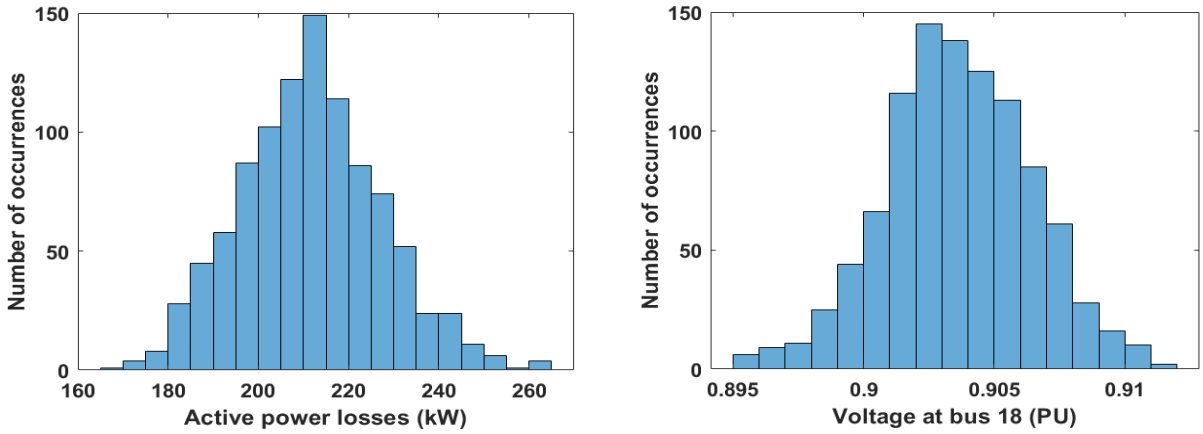

a) Active power losses

b) Per unit volatge at the minimum voltage bus

Fig. 20 Number of occurrences of the results for first system for Scenario 3

a. The results of the real system:

The same three previous scenarios are applied to the real system and the obtained results are listed in the following subsections.

For **Scenario** 1: The histograms of active power losses and voltage at bus 22 are recorded as shown in Figs. 21a and 21b, respectively. The active power losses are in the range [78-93] kW with a probability of 66.1% where the maximum probability percentage of 14.8% is prospective with active power losses of 82.5 kW as shown, in Fig. 21a. In addition, the maximum and minimum active power losses are prospective to be 110 kW and 64.5 kW with a probability of 0.2% and 0.3%, respectively.

The voltage at bus 22 is in the range [0.941-0.947] PU with a probability of 63.6% whereas the maximum probability percentage of 11.9% is prospective with a value of 0.9435 PU as shown in Fig. 21b. In addition, the maximum and minimum expected values of the voltage at bus 22 are 0.9525 PU and 0.9365 PU with a probability of 0.4% and 0.8%, respectively.

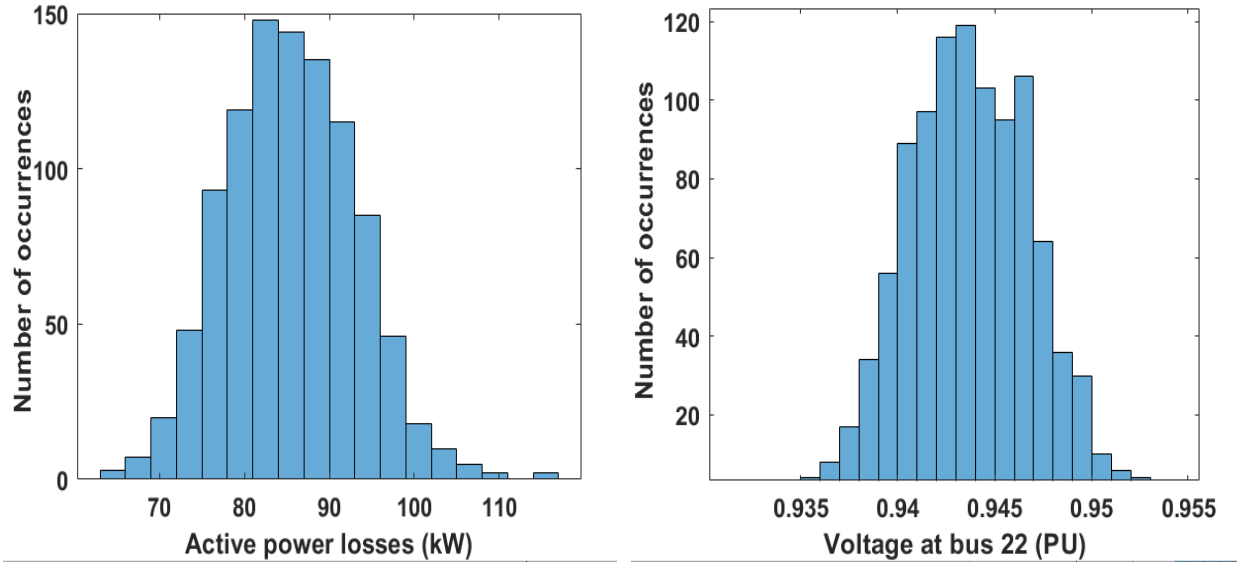

a) Active power losses b) Per unit volatge at the minimum voltage bus

Fig. 21 Number of occurrences of the results for the second system for Scenario 1

For **Scenario** 2: Fig. 22a shows the histogram of the active power losses at maximum loading condition which displays that they are in the range [60-70] kW with a probability of 67.1% where the maximum probability percentage of 16.6% is prospective with active power losses of 65 kW. In addition, the maximum and minimum active power losses are prospective to be 84 kW and 52 kW with a probability of 0.3% and 0.9%, respectively.

The histogram of the voltage at bus 22 at maximum loading condition is displayed in Fig. 22b which is in the range [0.95-0.955] PU with a probability of 66.2% where the maximum probability percentage of 15.6% is prospective with the value of 0.953 PU. In addition, the maximum and minimum expected values of the voltage at bus 22 are 0.96 PU and 0.944 PU with a probability of 0.4% and 0.2%, respectively.

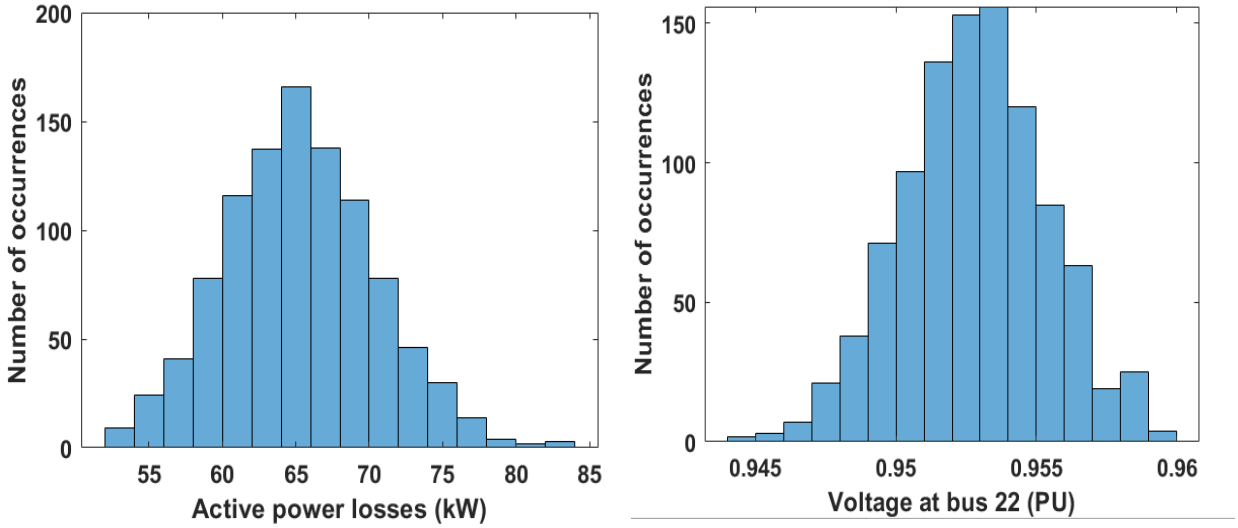

a) Active power losses b) Per unit volatge at the minimum voltage bus

Fig. 22 Number of occurrences of the results for the second system for Scenario 2

For **Scenario** 3: Fig. 23a shows the histogram of the active power losses at maximum loading condition which displays that they are in the range [72-87] kW with a probability of 69.4% where the maximum probability percentage of 15.5% is prospective with active power losses of 76 kW. In addition, the maximum and minimum active power losses are prospective to be 102 kW and 60 kW with a probability of 0.2% and 0.8%, respectively.

The histogram of the voltage at bus 22 at maximum loading condition is displayed in Fig. 23b which is in the range [0.942-0.949] PU with a probability of 73% where the maximum probability percentage of 11.6% is prospective with the value of 0.945 PU. In addition, the maximum and minimum expected values of the voltage at bus 22 are 0.954 PU and 0.935 PU with a probability of 0.7% and 0.1%, respectively.

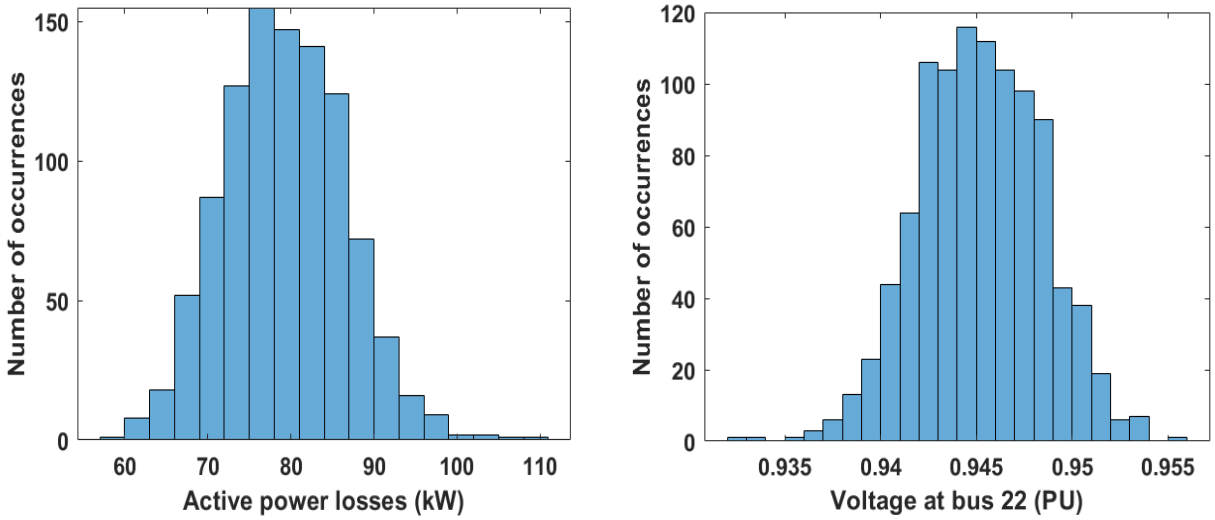

a) Active power losses b) Per unit volatge at the minimum voltage bus

Fig. 23 Number of occurrences of the results for the second system for Scenario 3

5. Results Discussion

The results demonstrated that: when load bus sensitivity factors are included, demand reduction can be more successful as observed when applying load reduction at the best feeder. Totally, it can be said that the proposed methodology has the ability to improve the performance of the distribution networks through noticeable improvements in the voltage profile, particularly the lowest voltage buses, as well as a reduction in system active power losses. The simulation results demonstrated that the methodology has the ability to present benefits for public companies in terms of reducing power taken from the grid and the production side. So, DSM can change the thinking of constructing a new plant to meet the demand and defer high investment to set up transmission and distribution networks.

6. Conclusions

This study depends on ranking the buses according to their sensitivity to network variations and classifying the feeders as the best and the worst feeders to apply DSM techniques to obtain the best systems performance. The hourly loading variations as well as their uncertainties are analyzed. The proposed methodology is applied to two distribution networks: an IEEE 33 standard system and a realistic distribution network. Three cases are investigated: the first employs DSM techniques to reduce the specified feeder loading by 20%. The second case used DSM techniques to reduce the specified feeder loading by 30% and the third is to study the uncertainties of the load by using Monte Carlo Simulation. It has been demonstrated that when load bus sensitivity factors are included, demand reduction can be more successful. This is accomplished through noticeable improvements in the voltage profile, particularly the lowest voltage buses, as well as a reduction in system active power losses. The results further confirmed that the suggested DSM technique may be used to avoid load shedding without causing excessive load reduction. The simulation results demonstrated that the methodology has the ability to present benefits for public companies in terms of reducing power taken from the grid and the production side. Furthermore, it is observed that the benefits of applying load demand reduction at the best feeder are high. Totally, it can be said that the proposed methodology has the proper performance in improving the efficiency of the distribution system.

7. References

[1] N. Alamir, S. Kamel, T. F. Megahed, M. Hori, and S. M. Abdelkader, "Developing Hybrid Demand Response Technique for Energy Management in Microgrid Based on Pelican Optimization Algorithm" Electric Power Systems Research, V. 214, January 2023.

[2] H. Karimi, G. Gharehpetian, R. Ahmadiahangar, and A. Rosin, "Optimal energy management of grid-connected multi-microgrid systems considering demand-side flexibility: A two-stage multi-objective approach" Electric Power Systems Research, V. 214, January 2023.

[3] http://www.moee.gov.eg/test_new/PDFReports/2020-2021-AR.

[4] S. Panda, P. K.Rout and B. K.Sahu, "Demand Side Management by PV Integration to Micro-grid Power Distribution System: A Review and Case Study Analysis" Green Technology for Smart City and Society, V.615, pp 417–432, 2020.

[5] A. Bolurian, H. Akbari, and S. Mousavi "Day-ahead optimal scheduling of microgrid with considering demand side management under uncertainty" Electric Power Systems Research, V.209, August 2022.

[6] A. M. Elsayed, M. M. Hegab, and S. M. Farrag, "Smart residential load management technique for distribution systems' performance enhancement and consumers' satisfaction achievement" International Transaction on Electrical Energy System, V. 29, No. 3, 2019.

[7] J. A. Saed, Z. Wari, F. Abughazaleh, J. Dawud, S. Favuzza, and G. Zizzo, "Effect of Demand Side Management on the Operation of PV-Integrated Distribution Systems "Applied Sciences, V. 10, No. 21, 2020.

[8] K. Kumar, and M. Gopichand, "Load Shifting Technique on 24Hour Basis for a Smart-Grid to Reduce Cost and Peak Demand Using Particle Swarm Optimization" International Research Journal of Engineering and Technology (IRJET), V. 4, No. 10, Oct 2017.

[9] N. R. Babu, T. Chiranjeevi, L. C. Saikia, and D. Raju, "Optimization Solutions for Demand Side Management" https://www.researchgate.net/publication/346145883, January 2021.

[10] E. Sarker, P. Halder, M. S. mahmoudian, E. Jamei, B. Horan, S. Mekhilef and A. Stojcevski "Progress on the demand side management in smart grid and optimization approaches "International Journal of Energy Research, 2020.

[11] C. Cecati, C. Citro, and P. Siano, "Combined operations of renewable energy systems and

responsive demand in a smart grid" IEEE Transactions on Sustainable Energy, V. 2, No. 4, pp. 468–476, 2011.
[12] E. Hartvigsson, J. Ehnberg, E. Ahlgren, and S. Molander, "Assessment of load profiles in minigrids: a case in Tanzania" International Universities International Universities Power Engineering Conference (UPEC), 2015.
[13] A. Barakat, A. Abaza, and A. M. Azmy, "Demand-Side Management to improve power system performance within smart grids environment" Engineering Research Journal Faculty of Engineering (ERJ) Menoufia University, 2014.
[14] M. Imani, P. Niknejad, and M. Barzegaran, "The impact of customers' participation level and various incentive values on implementing emergency demand response program in microgrid operation," International Journal of Electrical Power Energy Systems, V. 96, pp. 114–125, 2018.
[15] H. M. Hussain, N. Javaid, S. Iqbal, Q. Hasan, K. Aurangzeb and M. Alhussein, "An Efficient Demand Side Management System with a New Optimized Home Energy Management Controller in Smart Grid" Energies, V. 11, No. 1, 2018.
[16] G. H. Philipo, Y. A. Chande and T. Kivevele "Demand-Side Management of Solar Microgrid Operation: Effect of Time-of-Use Pricing and Incentives" Journal of Renewable Energy, 2020.
[17] H. Barry, H. G. Ignacio, C. Adam, H. Gareth, and D. Sasa, "Optimal Power Flow for Maximizing Network Benefits from Demand-Side Management "IEEE Transactions on Power System, V. 29, No. 4, 2014.
[18] B. N. Ram, V. Suvra, S. D. Saikia, and L. Chandra, "Scheduling of residential appliances using DSM with energy storage in smart grid environment" ICEPE, pp. 1–6, 2018.
[19] A. k. Sharma, A. Saxena, "A demand side management control strategy using Whale optimization algorithm" Springer Nature Journal, 2019.
[20] B. N. Ram, S. L. Chandra, and S. Debdeep, "Smart AC and micro-DC grid-based DSM using battery storage and wind energy" ICEPE, pp. 1–6, 2018.
[21] K. Sampath, and M. Sushama, "Strategic demand response framework for energy management in distribution system based on network loss sensitivity "Energy & Environment, 2020.
[22] M. Mohammed, A. Abdulkarim, A. S. Abubakar, A. B. Kunya, and Y. Jibril, "Load Modeling Techniques in Distribution Networks: a review" Journal of Applied Materials and Technology, V. 1, No. 2, pp. 63-70, 2020.
[23] A. A. Radwan, A. A. Z. Diab, A. H. M. Elsayed, H. H. Alhelou, and P. Siano, "Active distribution network modeling for enhancing sustainable power system performance; a case study in Egypt" Sustain, V. 21, pp.1–24, 2020, https://doi.org/ 10.3390/su12218991.
[24] A. Nasef, A. Shaheen, and H. Khattab, "Local and remote control of automatic voltage regulators in distribution networks with different variations and uncertainties: Practical cases study" Electric Power Systems Research, 2022.
[25] William H. Kersting, Distribution system modeling and analysis.
[26] K. D. Mistry, R. Roy, "Enhancement of loading capacity of distribution system through distributed generator placement considering techno-economic benefits with load growth" Int J Elect Power Energy Syst, V. 54, pp.505–15, 2014.
[27] J. Z. Zhu, "Optimal reconfiguration of electrical distribution network using the refined genetic algorithm" Elect Power Syst Res., V. 62, pp. 37–42, 2002.
[28] M. Kefayat, AL. Ara, and S. N. Niaki, "A hybrid of ant colony optimization and artificial bee colony algorithm for probabilistic optimal placement and sizing of distributed energy resources" Energy Convers Manage, V. 92, pp.149-161, 2015.
[29] A. M. Shaheen, E. E. Elattar, R. A. El-Sehiemy, and A. M. Elsayed, "An Improved Sunflower Optimization Algorithm-Based Monte Carlo Simulation for Efficiency Improvement of Radial Distribution Systems Considering Wind Power Uncertainty" IEEE Access, V. 9, pp. 2332–2344, 2021, doi:10.1109/ACCESS.2020.3047671.

APPENDIX

Table A shows the load and line data of Shebin El Kom feeder-Menoufia governorate-South Delta Electricity Company- Egypt.

TABLE A: Complete data of the studied system

Line	From	To	Length (Km)	R (Ω)	Type	Receiving PL (kW)	Receiving QL (kVAr)
1	1	2	0.73381	0.25228	C1	--------	--------
2	2	6	1.16788	0.4144	A	45.36	21.9744
3	6	7	1.00104	0.3552	A	144	69.76
4	7	9	0.66736	0.2368	A	576	279.04
5	9	11	0.58394	0.2072	A	--------	--------
6	11	12	1.08446	0.3848	A	45.36	21.9744
7	9	10	0.75078	0.2664	O3	115.2	55.808
8	7	8	0.66736	0.2368	O3	--------	--------
9	2	3	0.1772	0.04128	C2	72	34.88
10	3	4	0.50052	0.1776	O1	72	34.88
11	4	5	0.2215	0.0516	C2	72	34.88
12	6	13	0.58394	0.2072	O1	72	34.88
13	13	14	0.11075	0.0258	C2	360	174.4
14	13	15	0.66736	0.2368	A	45.36	21.9744
15	15	16	0.934304	0.33152	C2	--------	--------
16	16	17	1.00104	0.3552	O3	144	69.76
17	16	18	0.66736	0.2368	O2	--------	--------
18	18	19	0.33368	0.1184	O3	108	39.4144
19	18	20	0.8342	0.296	O3	--------	--------
20	20	21	1.00104	0.3552	O3	72	34.88
21	20	24	1.33472	0.4736	O2	72	34.88
22	24	22	0.66736	0.2368	C2	45.36	21.9744
23	22	23	0.33368	0.1184	C2	--------	--------
24	24	25	0.50052	0.1776	O3	18	8.72
25	25	26	0.4171	0.148	O3	--------	--------
26	26	27	1.00104	0.3552	O3	36	17.44
27	26	28	0.33368	0.1184	O3	45.36	21.9744

where

O1: Overhead transmission line, Aluminum Conductor Steel Reinforced (ACSR) with area equals 150/25 mm^2

O2: Overhead transmission line, Aluminum Conductor Steel Reinforced (ACSR) with area equals 70/12 mm^2

O3: Overhead transmission line, Aluminum Conductor Steel Reinforced (ACSR) with area equals 35/6 mm^2

A: Overhead transmission line, All Aluminum Alloy Conductor (AAAC) with area equals 70 mm^2

C1: Underground cable XLPE with area equals 3*300 mm^2

C2: Underground cable ALX with area equals 3*240 mm^2

C3: Underground cable ALX with area equals 3*150 mm^2

C4: Underground cable XLPE with area equals 3*70 mm^2